CHAPTER II
THEORETICAL BACKGROUND AND LITERATURE SURVEY

2.1 THEORETICAL BACKGROUND

2.1.1 Theory of Gas Transport in Membranes

The development of membranes for the separation and purification of gases based on the selective permeation of one or more components of a mixture has attracted considerable interest during the last decade. There are three types of polymeric membranes based on the mechanism of gas separation. The first is a porous membrane which uses a molecular sieve to separate one type of molecule from another type, based on the size of the molecules. The molecules which are larger than the pore of the membrane cannot move across the membrane to the permeate side but are rejected and stay at the retentate side of the membrane. The second is a nonporous membrane or dense membrane. Its separation behavior follows the solution-diffusion model (Figure 2.1).

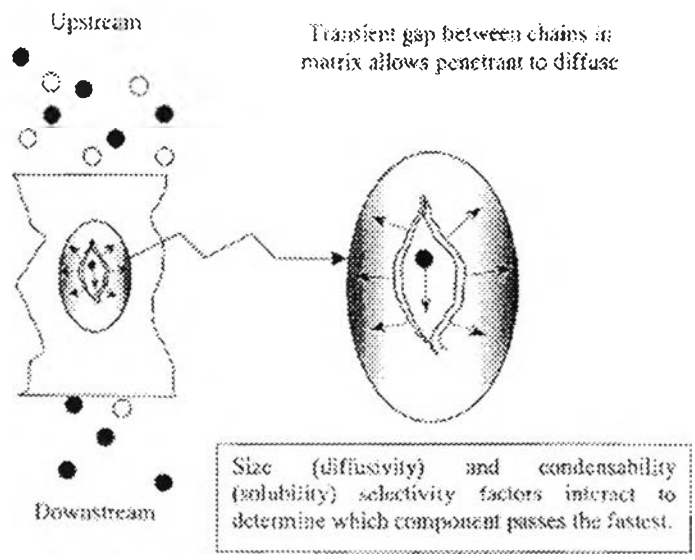

Figure 2.1 Solution-diffusion mechanisms (From Ismail *et al.*, 2002).

The separation is achived between the different permeants because of differences in the amount of material diffusing through the membrane and the rate at

which the material diffuses (Wijmans *et al.*, 1995). The mechanism occurs in three successive steps: (1) sorption of the penetrant in the polymer film; (2) diffusion of the penetrant through the polymer film; and (3) desorption at the opposite interface. This solution-diffusion model is widely used in gas separation applications to control the permeation of different species. The chemical potential gradient across the membrane is expressed as a concentration gradient, but not a pressure gradient (Ismail *et al.* 2002). The third type is called an asymmetric membrane (Figure 2.2) which consists of two layers: a very thin, selective, dense layer on the top surface and a thick, porous support on the other side. The latter is effective for both a high permeation rate and the mechanical support given to the thin selective layer.

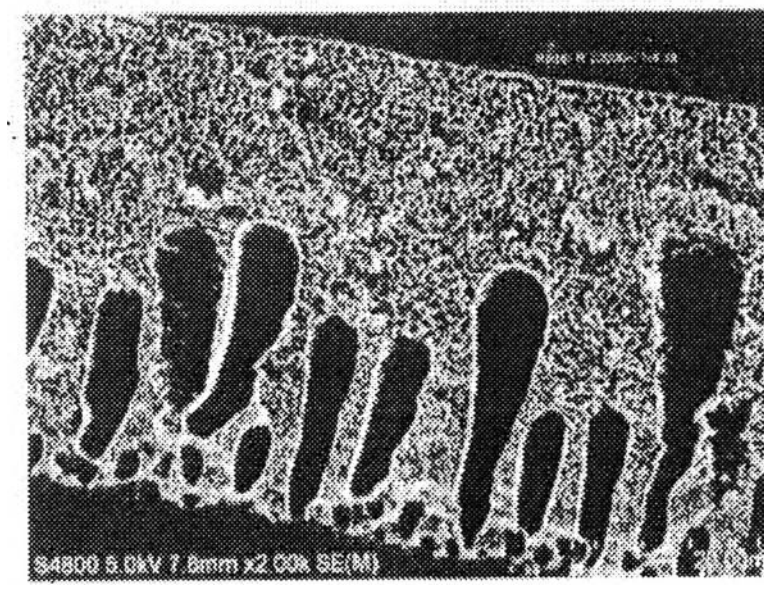

Figure 2.2 Asymmetric membrane (From Zhang *et al.*, 2006).

The thin selective membrane is essential in the separation of small molecules by the membrane system. Therefore, to understand the asymmetric membrane's transport properties, studies on sorption, diffusion, and permeation of gas through the dense membrane must be done.

The permeation of a penetrant through a polymer membrane for gas separation is described by a permeability coefficient P, which is defined as the flux,

N, divided by the difference in pressure of the penetrant between upstream and downstream, Δp, and membrane thickness, l:

$$P = \frac{N}{(\Delta p)/l} \tag{2.1}$$

According to the solution-diffusion model, the permeability, P, can be written as a product of solubility coefficient S, and a kinetic parameter, called the diffusion coefficient, D:

$$P = DS \tag{2.2}$$

Therefore, gas permeability is not a fundamental property of these materials. It is the product of a mobility (kinetic)-related term and a solubility (thermodynamic)-related term. The diffusion coefficient is a measure of the mobility of the penetrants between the upstream and downstream conditions on the membrane. It depends on the packing and motion of the polymer segments and on the size and shape of the penetrating molecules. The solubility coefficient is determined by the condensability of the penetrant, the extent of the polymer-penetrant interaction, and the amount of free volume existing in the polymer (Staudt-Bickel and Koros, 2000).

The ability of a membrane to separate a gaseous mixture of A and B in a single-stage membrane process may be characterized by the ideal separation factor or permselectivity, $\alpha_{A/B}$. In the case where the downstream pressure is negligible compared to the upstream pressure, the separation factor $\alpha_{A/B}$ is simplified to:

$$\alpha_{A/B} = P_A/P_B \tag{2.3}$$

where P_A and P_B are the permeabilities of pure gases A and B, respectively.

The term $\alpha_{A/B}$ can be written as the product of the diffusivity selectivity and the solubility selectivity of the gas pair:

$$\alpha_{A/B} = \frac{D_A}{D_B} \times \frac{S_A}{S_B} \tag{2.4}$$

where D_A/D_B is the diffusivity selectivity and S_A/S_B is the solubility selectivity. The diffusivity selectivity reflects the different sizes of two molecules. The solubility selectivity is controlled by the difference of the condensabilities of the two penetrants and the physical interaction of the penetrants with the particular polymer membrane

2.1.2 Effect of carbon dioxide on polymer plasticization

2.1.2.1 Gas-polymer interactions

It is well known that CO_2 acts as a plasticizer at a sufficiently high level of concentration (Petropoulos, 1992). CO_2 has a quadrupole moment and is probably more soluble in polymers with a polar matrix. Also, high gas solubilities can be attributed to the plasticization of the polymer matrix, and the penetrants can lead to low gas diffusivities (Costello and Koros, 1992). Small amounts of sorbed CO_2 cause changes in the polymer chain packing which increases the frequency of the main-chain molecular motion of the polymer, confirmed by C-13 NMR measurement (Sefick and Schaefer, 1983). The strong interaction between CO_2 and basic sites in polymers permit a higher degree of plasticization, which decrease interchain interactions with a consequent increase in the free volume of the polymer. It has been suggested that the CO_2-polymer interaction may be of Lewis acid-base type. CO_2 serves as a Lewis acid (electron acceptor) in the presence of a basic polymer group (electron donor) (Kazarian *et al.*, 1999).

2.1.2.2 CO_2-permeation behavior

In general, the CO_2-permeability characteristics of glassy polymers can be categorized into three types, as shown in Figure 2.3.

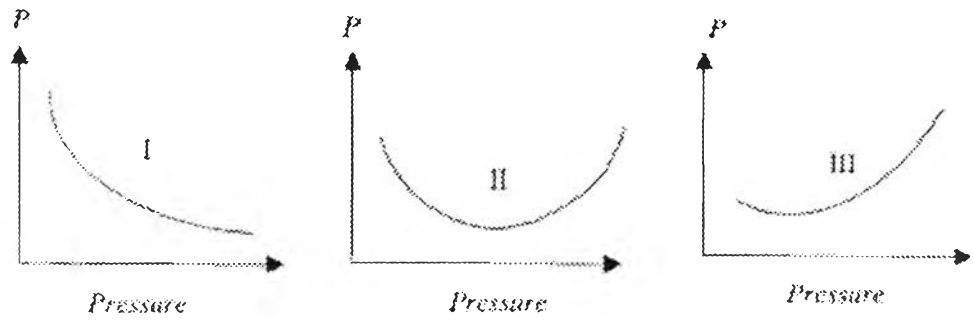

Figure 2.3 Representation of the possible shapes of the permeability (P) of several glassy polymers to CO_2 (Ismail. A.I., and Lorna, W. 2002).

Type I. The gas permeability of the polymer continuously decreases with increasing pressure. This type of polymer does not have large substituents on the backbone; for example, polysulfone and polycarbonate for pressures up to 30 bar.

Type II. The permeability decreases with increasing the pressure at low feed pressure. When the pressure is increased to a critical pressure, the permeability of gas begins to increase with increasing pressure; for example, various polyimides.

Type III. For polyarylate and cellulose acetate (CA); they have permeability to CO_2 that gradually increases as a function of pressure. Even though these polymers are glassy polymers, they exhibit a similar permeation behavior as found for rubbers.

Referring to the solution-diffusion model, the increase in permeability is mainly attributed to the concentration dependence of the diffusion coefficient. The pressure dependence on solubility coefficient is similar for different polymers. For this reason, differences in permeability are determined mainly by the diffusivity. In addition, the diffusivity normally increases with increasing pressure, while the solubility decreases. Because the diffusion coefficient increases with concentration much more rapidly than the solubility coefficient decreases with pressure, an increase in permeability is therefore feasible. However, this does not mean that the solubility of a penetrant is not important, but solubility indirectly contributes to the increase in diffusivity. The diffusion coefficient can only increase because the CO_2 concentration in the polymer increases.

2.1.3 Plasticization in asymmetric membranes

Donohue *et al.* (1989) studied the anomalous permeation behavior for CO_2 and CH_4 of an asymmetric cellulose acetate membrane. This strange behavior was explained by the plasticization phenomena. Test results also showed that the CO_2 permeability rate and the methane permeability rate rapidly increase with the increase in operation temperature and pressure.

Jordan *et al.* (1990) investigated the effect of CO_2 on the permeation behavior of asymmetric hollow fiber membranes and dense films composed of an aromatic polyimide from the reaction of 6FDA dianhydride and aromatic diamine. Experimental data showed that an asymmetric membrane conditioned with CO_2 in-

creased air permeation rates greater than dense films. This considerable difference occurred due to a change in the supramolecular morphology of asymmetric membranes. Figure 4 illustrates the explanation of CO_2 conditioning effects on the dense skin morphology of asymmetric hollow fibers.

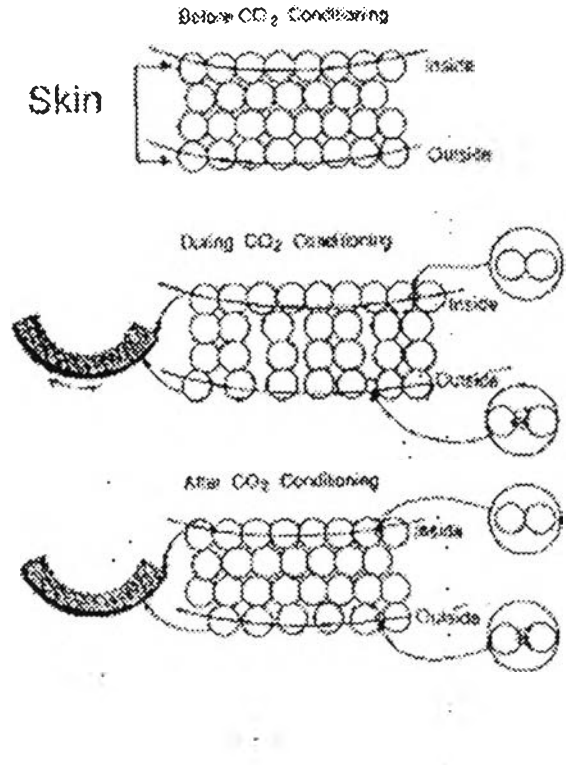

Figure 2.4 Hypothetical explanation of CO_2 conditioning effects on dense skin morphology of symmetric hollow fiber membrane (Jordan et a.l 1990).

The authors proposed that 'tie chains' become interconnectors when these tie chains between nodules partially separate, determined by the CO_2 sorption level or the chain stability. They also proposed that there are two important factors which influence the permeability of the hollow fiber module: (i) swelling of the glassy matrix within the nodules owing to highly soluble CO_2, and (ii) decrease of the effective dense skin thickness.

2.1.4 Permeation model of MMMs

2.1.4.1 History of mathematical modeling of gas permeation through MMMs (Bouma et al., 1997),

The permeation of gases through MMMs, in which solid adsorbents are dispersed, has been exhaustively studied by experimentalists and theorists. It is obvious that, to describe the permeability of MMMs, an equation which correlates the permeability of continuous phase and the dispersed phase, and the amount of dispersed particles is needed.

From principle, there is analogy between the permeability coefficient of gases that pass through MMMs and dielectric permittivity of dielectric materials in heterogeneous systems. In dielectric materials, the negative gradient of the electrical potential ϕ, which is also called the electric field (E), is a driving force for electric current. The electric displacement (D) is proportional to the electric field, and the proportional factor is defined as the dielectric constant or permittivity ε. In case of dielectric materials that consist of two or more phases, it is usually assumed that, at least in theoretical point of view, the electrical potential is smoothly changed across any interface between arbitrary phases. In the same way, the negative gradient of the pressure (p) is the driving force for gas permeation through membrane. The flux (J) is proportional to the negative gradient of pressure with proportional factor called the permeability coefficient (P). Like the electrical potential, the pressure is also assumed that it smoothly changes across any interface between two phases. The comparison between dielectric permittivity of dielectrics material and gas transport through membranes is given below.

Driving force:	$E = -\nabla\phi$ vs. ∇p	(2.5)
Flux:	$D = -\varepsilon\nabla\phi$ vs. $J = -P\nabla p$	(2.6)
Interface:	ϕ is continuous vs. p is continuous	

Therefore, any solutions derived for the apparent dielectric permittivity of a heterogeneous system can be directly applied to the permeability of gas through MMMs by replacing the dielectric permittivity of the continuous and dis-

persed phases with the permeability or permeance of gas in the respective phases.

2.1.4.2 Mathematical modeling of gas permeation through MMMs (Gonzo et al., 2006 and Pal, 2007)

The minimum and maximum values of the effective permeability of a given penetrant P_{eff}, in MMMs are given by the series and parallel two-layer models, respectively. The minimum value of P_{eff} occurs when a series mechanism of gas transport through the continuous and dispersed phases is assumed:

$$P_{eff} = \frac{P_c P_d}{\phi_c P_d + \phi_d P_c} \tag{2.7}$$

The maximum value of P_{eff} is obtained when continuous and dispersed phases are assumed to work in parallel to the flow direction:

$$P_{eff} = P_c \phi_c + P_d \phi_d \tag{2.8}$$

The geometric mean model assumes random distribution of both phases (continuous and dispersed phases). The effective permeability is given by the weighted geometric mean of the permeabilities of the two matrixes;

$$P_{eff} = P_c^{\phi_c} + P_d^{\phi_d} \tag{2.9}$$

, where P_c and ϕ_c are defined as the permeability of a given penetrant in the continuous and volume fraction of continuous phases, respectively. In the same way, P_d and ϕ_d are labeled as the permeability of a given penetrant in the dispersed phase and volume fraction of dispersed phases.

Maxwell used the potential theory to explain the electrical conduction through a heterogeneous media, and he obtained the exact solution for the conductivity of random distributed and non-interacting homogeneous solid spheres in a continuous matrix. As mentioned above, Maxwell equation for dielectric material can be adapted to the gas permeation problems by replacing the dielectric permittivity of the continuous and dispersed phases with the permeability or permeance of gas in the respective phases. Maxwell equation is expressed as;

$$P_{eff} = P_c \left(\frac{P_d + 2P_c - 2\phi(P_c - P_d)}{P_d + 2P_c + \phi(P_c - P_d)} \right) \tag{2.10}$$

, where ϕ is volume fraction of the dispersed phases and n is the shape factor of the dispersed phase.

Maxwell equation can write in another way as;

$$P_{eff} = P_c\left(\frac{2(1-\phi)+\alpha(1+2\phi)}{(2+\phi)+\alpha(1-\phi)}\right) \tag{2.11}$$

, where $\alpha = \frac{P_c}{P_d}$.

It is very useful to define the reduced permeation polarizability β as:

$$\beta = \frac{\alpha-1}{\alpha-2} = \frac{P_d - P_c}{P_d + 2P_d} \tag{2.12}$$

Parameter β measures the difference in penetrant permeability between the continuous and dispersed phases. The value of β is bounded by $-0.5 \leq \beta \leq 1$. Where the lower limits correspond to totally nonpermeable and the upper limits represents the case of perfectly permeable dispersed phased. When β = 0, it implies α = 1 (equal permeability in continuous and dispersed phases). Maxwell equation can be written as a function of β as shown in below:

$$P_{eff} = P_c\frac{1+2\beta\phi}{1-\beta\phi} \tag{2.13}$$

Because of the assumption that the flux pattern around a dispersed particle is not disturbed by the presence of other dispersed particles, Maxwell equation is only applicable to the dispersions that have low volume fraction (≤20%) of dispersed particles. Nevertheless, many published results show that Maxwell equation can applied in case of high volume fraction. It should be noted that Maxwell equation does not have any parameter. Moreover, the problem with Maxwell model lies in its neglect of the interactions between the dispersed particle and the polymer chains, and the dispersed particle and the penetrants. In most MMMs, these interactions usually strong and significantly change the diffusivity and solubility characteristic of penetrants.

Above equation is an analytical solution that can be also obtained by embedding one unit cell of the dispersed phase in the continuous phase. By solving the Laplace equation of the pressure in both the continuous and dispersed phase and applying the boundary condition that there is no accumulation of gas species in the dispersed-continuous and the continuous-mixed matrix interface, will give Maxwell-Wagner-Sillars equation:

$$P_{eff} = P_c \frac{nP_d + (1-n)P_c + (1-n)(P_d - P_c)\phi}{nP_d + (1-n)P_c - n(P_d - P_c)\phi} \qquad (2.14)$$

, where n is shape factor.

For prolate dispersed particle, i.e. the longest axis of the particle is directed along the applied pressure gradient, the value of parameter; n is between 0 and 1/3. In case of spherical filler particle, n is equal to 1/3. For oblate dispersed particle, i.e. the shortest axis of the particle is directed along the applied pressure gradient; n is between 1/3 and 1. In special case, n = 0, 1/3, and 1, Maxwell-Wagner-Sillars equation gives:

$$n = 0 : P_{eff} = P_c(1-\phi) + P_d\phi_d, \qquad (2.15)$$

$$n = 1/3 : P_{eff} = P_c \frac{P_d(1+2\phi) + P_c(2-2\phi)}{P_d(1-\phi) + P_c(2+\phi)}, \qquad (2.16)$$

$$n = 1 : P_{eff} = P_c \frac{P_d}{P_d(1-\phi) + P_c\phi} \qquad (2.17)$$

It should be noted that Maxwell-Wagner-Sillars equation has the ability to predict the gradual changing of gas permeation through a membrane with parallel transport (n = 0) to permeation through a stack of layers (n = 1). In case of n=1/3, the obtained equation called Maxwell equation as already mentioned. This means that Maxwell equation is a special case of Maxwell-Wagner-Sillars equation.

Bruggeman used the effective medium theory approach, which is particularly suitable when there is a difference in the permeability of the two phases is small ($\alpha \approx 1$). Because of the effective medium theory treats the local permeability as fluctuations about the effective permeability of a uniform medium, no distinction between continuous and dispersed phases is made. He made his equation valid at low volume fraction of filler and assumed that this equation can be used for calculating

the infinitesimal increment of the dispersion dielectric constant after adding an infinitesimal amount of the filler. The infinitesimal increment of the filler volume fraction is integrated to get an equation for the dielectric constant at relatively high filler volume fractions. Thus, Bruggeman equation is also valid at high volume fraction of filler also. Bruggeman equation for gas permeation through a dispersion of spherical particles is:

$$\left(\frac{P_{eff}}{P_c}-1\right)\left(\frac{P_{eff}}{P_c}\right)^{-1/3}=(1-\phi)(1-\alpha) \tag{2.18}$$

Bottcher and Higuchi derived an expression that can be applied to the case of random dispersions of spherical particles. Bottcher equation is:

$$\left(1-\frac{P_c}{P_{eff}}\right)\left(\alpha+2\frac{P_{eff}}{P_c}\right)=3\phi(\alpha-1) \tag{2.19}$$

Higuchi equation is:

$$\frac{P_{eff}}{P_c}=1+\frac{3\beta\phi}{\left[1-\phi\beta-K_H(1-\phi)\beta^2\right]} \tag{2.20}$$

Parameter K_H in Kiguchi equation is an empirical constant which is assigned a value of 0.78 based on experimental data. It is obvious that Bottcher and Higuchi equations are third order and second order algebraic expressions in P_{eff}, so a trial and error procedure is needed to calculate P_{eff} as function of α and ϕ.

Refer to the percolation theory, the relation between composite permeability and filler concentration in the vicinity of the percolation threshold can be described by a simple power law:

$$P_{eff}=P_d(\phi-\phi_t)^t \tag{2.20}$$

Where ϕ_t is the percolation threshold or critical volume fraction of the filler, and t is the critical exponent. Based on this approach, expanding Maxwell equation which written in term of β and ϕ yields:

$$\frac{P_{eff}}{P_c}\approx 1+3\phi\beta+3(\phi\beta)^2+O(\phi^3) \tag{2.21}$$

The second term illustrates the interaction between dispersed particles and continuous phase and the third term represents the interaction between particles.

Mathematically speaking, P_{eff} of a homogeneous dispersion is a statistical property that depends on the nature and permeating properties of the continuous and disperse phases and on the spatial distribution of the particles in the mixed matrix material. However, it is convenient to explain or describe the permeation system behavior with only two parameters β and ϕ. Nevertheless, in many experiments, ϕ is usually regarded as a single parameter used to describe an ensemble of identical spheres of dispersed phase which interact with the continuous media and also with them.

As discussed above, Maxwell equation neglects particle to particle interactions, and assumed that effect of the particle size was negligible when compared with mean free path within particles. By taking the original Maxwell equation, Chiew and Glandt proposed:

$$\frac{P_{eff}}{P_c} \approx \frac{1+2\beta\phi+\left(K-3\beta^2\right)\phi^2}{1-\beta\phi}+O\left(\phi^3\right), \tag{2.22}$$

An expansion of this expression in terms of ϕ yields:

$$\frac{P_{eff}}{P_c} \approx 1+3\phi\beta+K\phi^2+O\left(\phi^3\right) \tag{2.23}$$

K values were calculated by using appropriated statistical functions to describe the interaction of the "ith" particle with the surrounding ensemble and integration to sum up all the resulting interaction contributions. K is not only a function of β but also of ϕ, as expected. By fitting to the experimental data give following expressions for K values:

$$K = a + b\phi^{3/2} \tag{2.24}$$

, where the parameter a and b are functions of β.

$$a = -0.002254 - 0.123112\beta + 2.93656\beta^2 + 1.6904\beta^3 \tag{2.25}$$

$$b = 0.0039298 - 0.803494\beta - 2.16207\beta^2 + 6.48296\beta^3 + 5.27196\beta^4 \tag{2.26}$$

When $\phi \ll 1$, Chiew and Glandt equation give the same results as Maxwell predictions since terms of order ϕ^2 will be negligible in comparison with terms of order ϕ. However, it should be noted that Brudgeman and Bottcher expressions also reduces to Chiew and Glandt equation up to terms of order ϕ.

The Lewis-Nielsen model, primarily proposed for the elastic modulus

of particulate composites, can be adapted to permeability as:

$$P_{eff} = P_c \left(\frac{1 + 2\phi\left(\frac{\alpha - 1}{\alpha + 2}\right)}{1 - \psi\phi\left(\frac{\alpha - 1}{\alpha + 2}\right)} \right) \tag{2.27}$$

Where,

$$\psi = 1 + \left(\frac{1 - \phi_m}{\phi_m^{\,2}} \right)\phi \tag{2.28}$$

ϕ_m is the maximum packing volume fraction of filler particles, e.g. zeolite particle (ϕ_m is typically equal to 0.64 for random close packing of uniform spheres).

The Lewis-Nielsen model predicts the right behavior at $\phi \rightarrow \phi_m$. However, the relative permeability, P_r, at $\phi=\phi_m$ diverges when the permeability ratio α approaches infinity. The Lewis-Nielsen model also includes the effects of morphology on permeability through parameter ϕ_m which is sensitive to particle size distribution, particle shape, and aggregation of particles. As $\phi_m \rightarrow 1$, the Lewis-Nielsen model reduces to Maxwell model.

Originally, Pal model derived to explain thermal conductivity of particulate composites can be adapted to permeability as:

$$\left(\frac{P_c}{P_m}\right)^{1/3} \left(\frac{\alpha - 1}{\alpha - \left(\frac{P_c}{P_m}\right)} \right) = \left(1 - \frac{\phi}{\phi_m}\right)^{-\phi_m} \tag{2.29}$$

The Pal model was developed using the differential effective medium approach taking into consideration the packing difficulty of filler particles. Notice that when $\phi_m \rightarrow 1$, the Pal model reduces to the Bruggeman model. The Pal model, similar to the Lewis-Nielsen model, gives the correct behavior at $\phi \rightarrow \phi_m$. It also takes the effects of morphology on permeability into account through the parameter ϕ_m (ϕ_m is sensitive to morphology). Though, the Pal model, like the Bruggeman model, is an implicit relationship that needs to solve numerically for P_{eff}.

Table 2.1 summarizes the existing permeation models, the variables

appeared in this table have previously defined and also have the same meaning as discussed above.

Table 2.1 Summary of existing permeation model.

Model	Equation
Maxwell	$P_{eff} = P_c \frac{1 + 2\beta\phi}{1 - \beta\phi}$
Bruggeman	$\left(\frac{P_{eff}}{P_c} - 1\right)\left(\frac{P_{eff}}{P_c}\right)^{-1/3} = (1 - \phi)(1 - \alpha)$
Bottcher	$\left(1 - \frac{P_c}{P_{eff}}\right)\left(\alpha + 2\frac{P_{eff}}{P_c}\right) = 3\phi(\alpha - 1)$
Higuchi	$\frac{P_{eff}}{P_c} = 1 + \frac{3\beta\phi}{\left[1 - \phi\beta - K_H(1 - \phi)\beta^2\right]}$
First order Maxwell–Wagner–Sillar	$\frac{P_{eff}}{P_c} \approx 1 + 3\phi\beta$
Second order Maxwell–Wagner–Sillar	$\frac{P_{eff}}{P_c} \approx 1 + 3\phi\beta + 3(\beta\phi)^2$
Chiew and Glandt	$\frac{P_{eff}}{P_c} \approx 1 + 3\phi\beta + K\phi^2$
Lewis-Nielsen	$P_{eff} = P_c\left(\frac{1 + 2\phi\left(\frac{\alpha - 1}{\alpha + 2}\right)}{1 - \psi\phi\left(\frac{\alpha - 1}{\alpha + 2}\right)}\right)$
Pal	$\left(\frac{P_c}{P_m}\right)^{1/3}\left(\frac{\alpha - 1}{\alpha - \left(\frac{P_c}{P_m}\right)}\right) = \left(1 - \frac{\phi}{\phi_m}\right)^{-\phi_m}$

2.2 LITERATURE REVIEW

2.2.1 Polymeric Membranes

In 1960, Leob and Sourirajan invented the asymmetric integrally skinned cellulose acetate reverse osmosis membrane. These workers invented the first asymmetric, integrally skinned cellulose acetate RO membranes. These membranes were 10 times higher in flux than that of any membrane then available and made RO applications viable. Subsequent progress in membrane science and technology was focused on the development and refinement of these concepts. As a result, many commercial processes (such as microfilltration, ultrafilltration RO, and electrodialysis) were all established; but not gas separation. Though the advantages are a simple flow configuration and low-maintenance operation, membrane systems cannot compete with the adsorption systems for most gas separation applications because of their low selectivity and flux. The separation of gas mixtures of industrial interest with polymeric membranes became economically feasible in the late 1970s for certain applications like the removal of hydrogen gas from the product stream of ammonia using the Monsanto Prism membrane. Cynara and Separex Company employed membranes for the separation of carbon dioxide.

There are two types of polymeric membranes that are widely used commercially for gas separations. Glassy polymeric membranes are rigid and glass-like, and operate below their glass transition temperatures (T_g). Rubbery polymeric membranes are flexible and operate above their glass transition temperatures. In general, polymeric membranes exhibit inverse permeability/selectivity behavior. In other words, selectivity to given penetrant pair increases as the gas permeability through it decreases (Stern, 1994). Rubbery polymers typically show a high permeability, but a low selectivity, whereas glassy polymers exhibit a low permeability but a high selectivity. Glassy polymeric membranes dominate industrial membrane separations because of their higher gas selectivities, in addition to better mechanical properties compared to that of rubbery polymers. Poly(dimethylsiloxane) (PDMS), silicone polymer, is only rubbery polymers that used in gas separations. Glassy polymers such as polyacetylenes, poly[1-(trimethylsilyl)-1-propyne] (PTMSP), polyimides, polyamides, polycarbonates, polysulfones, cellulose acetate, poly(phenylene oxide)

are polymeric material that widely used for gas separations. In this section will be focused on literatures which involve glassy polymeric membrane only.

Gantzel and Merten (1970) prepared fully dense cellulose acetate (CA) from casting solution. The resulted membranes permit high gas permeation rate. They also found trade-off between permeability and selectivity.

Minhas *et al.* (1987) fabricated cellulose acetate membranes by solution casting method at different shrunk temperature. The membranes were tested at room temperature for separation CO_2/CH_4 mixtures. The permeation rate was widely varied in the range of 0 to 1.33×10^{-4} kmol/m^{2}s. They suggested that the shrinkage temperature strongly influence the membrane performance for CO_2/CH_4 mixtures separation.

Matsumoto *et al.* (1993) prepared two hexafluoro-substituted aromatic polyimides, 6-FDA-p-PDA and 6FDA-4,4'-ODA, for gas permeation studies. They attained higher gas permeabilities through 6FDA polyimides, compared with PMDA polyimides, while high permselectivities of 6FDA polyimides were retained. They explained that a helix configuration due to the bulky $-C(CF_3)_2-$ group in the polymer backbone contributes to the increase in the free volume of the polymer, therefore, it regulates the gas diffusivity.

Costello *et al.* (1994) studied hexafluorodianhydride-3,3',4,4'-tetraaminodiphenyl oxide (6FDA-TADPO), polypyrrolone material, for membrane-based gas separations at higher temperatures. They talked about the loss of permselectivities of various gas pairs with increasing temperature in terms of both solubility selectivity and diffusivity selectivity. They scrutinized that the solubility selectivity of gas pairs with the 6FDA-TADPO membrane was not affected by increasing temperature. So, the loss of permselectivities should come from the loss of the diffusivity selectivity at elevated temperature. They concluded that the diffusivities of larger molecules promote more from increased polymer chain motion due to increasing temperature. The CO_2/CH_4 (size difference 0.5 A) permselectivity decreased more quickly with the increase in temperature than the CO_2/N_2 (size difference 0.34 A) permselectivity.

Okamoto *et al.* (1993 and 1995) studied gas permeation properties of poly(ether imide) segmented copolymer films prepared from polyether-diamine, co-monomer diamine, and acid anhydride. The poly(ether imide) segmented copolymers have microphase-separated structures consisting of microdomains of rubbery poly-ether segments used for the gas permeation and of glassy polyimide segment for the mechanical properties and film forming ability. The copolymer films having PEO content of about 70 percent by weight showed high CO_2 permeance (140 Barrer) with a CO_2/N_2 permselectivity of 70 at 25 °C. The PEO containing polyimide membranes also exhibited both high permeability of CO_2 (75 Barrer) and high separation factor of CO_2/ N_2 (equals to 65) at 25 °C for a CO_2-N_2 mixture containing 18 percent CO_2. They accredited the high permselectivity to the high solubility selectivity resulting from the high affinity of CO_2 to PEO segments.

Hirayama *et al.* (1996) examined the relation of gas permeabilities, diffusivities, and solubilities with the structures of various polyimide films. They summarized that the diffusivities of amorphous polyimides do not correlate with the intersegmental spacing parameters (d-spacing and fractional free volumes), especially for polyimides containing polar substituents.

Suzuki *et al.* (1998) fabricated composite hollow fiber membranes composed of a thin and dense outer-layer of BPDA-PEO/ODA polyimide and a sponge-like layer of BPDA-ODA/DABA polyimide. The 1 mm thick outer layer was accountable for the gas separations. They had same results from mixed gas measurement, as well as from pure gas measurement. The CO_2 permeance and the CO_2/N_2 permselectivity decreased in a month after the membrane preparation. The reduction of membrane performance was caused by densification of the inner layer at the interface to the outer layer, which might be caused by a plasticization effect of the PEO-containing polyimide. For this reason, the interface of the inner layer might become dense and act as an additional layer. Though, the membrane performance did not change a lot subsequent to the first month.

Kim *et al.* (2001) made pore-filled membranes by using polyacrylonitrile membrane as a support and methoxy poly(ethylene glycol) acrylate (MePEGA) as a filler by UV-irradiated photografting. They archived high CO_2/ N_2 permselectiv-

ity (32.5) with very low CO_2 permeability (5.65×10^{-4} Barrer) from this pore-filled membrane at a temperature of 30 °C.

Poly(ethylene glycol) (PEG) can dissolve substantial amounts of acidic gases, and the gas diffusivity in the PEG segment may be high, since the chain is flexible. It is very difficult to obtain a thin film of PEG with mechanical and thermal stability. Therefore, highly stable membranes are obtained by blending PEG with other polymers, where the PEG segment provides high permeability coefficients and high permselectivities, and the other polymers provides robustness to the membranes.

M. Kawakami *et al.* (1982) also reported cellulose nitrate/PEG blend membranes having up to 50 percent by weight of PEG. These membranes showed CO_2 permselectivities of 29 to 38, with CO_2 permeabilities of 1.4-8.2 Barrer. The permeability and CO_2 permselectivity of cellulose nitrate/PEG blended membranes increase appreciably with increasing PEG fraction. The significant increase in CO_2 permeability was attributed to the increments to both diffusivity and solubility of CO_2. It has been interpreted that an increase in diffusivity results from the spreading effect of the PEG plasticizer on the polymer chain.

Li *et al.* (1998) fabricated poly(ethylene glycol) (PEG)/cellulose acetate (CA) blended membranes for gas permeation studies. The apparent solubility coefficients of CO_2 were reduced by blending PEG20000 (average molecular weight of 20,000). The blended membranes containing PEG exhibited high apparent CO_2 diffusivity coefficients, resulting in high permeability coefficients for CO_2 compare to that of the CA membrane. They described that flexible main chain of PEG20000 in the amorphous domains in the blends permitted the large penetrants, CO_2, and CH_4 to diffuse easily through the blended membranes, resulting in higher permeance of CO_2, and CH_4 relative to that of N_2. Hence, the CO_2/ CH_4 permselectivities decreased by blending of PEG20000 with CA.

2.2.2 Mixed Matrix Membranes (MMMs)

To increase the membrane selectivity, either the diffusivity selectivity or solubility selectivity needs to be enhanced. However, for a particular polymer membrane, these factors are fixed and difficult to change without chemically modifying the molecular structure.

Chemical modification of the polymer membrane can be achieved for gas separation. However, selectivity enhancement through a gas diffusion mechanism is still difficult. This is because of the small difference in the kinetic diameter of each molecule to be separated.

To enhance the commercial applicability of polymer membrane separation processes, Kulprathipanja and coworkers at UOP LLC (1986 and1988) developed the mixed matrix membrane (MMM) that allows the membrane selectivity to be increased through gas solubility optimization.

Two types of MMMs have been developed. The first is a membrane with an adsorbent embedded in the polymer matrix (MMM_{ADS}). The polymers can be cellulose acetate (CA), polysulfone, polyether sulfone, polyimide, or a rubbery polymer such as silicone rubber. The adsorbent can be zeolite–such as NaX, AgX, NaY, NaA–silicalite, silica gel, alumina or activated carbon.

The second type of MMM is fabricated by casting polyethylene glycol (PEG) and silicone rubber on a porous polysulfone support (MMM_{PEG}).

Both types of MMMs can be used in commercial gas separation processes, such as the separation of polar gas from non polar gas, carbon dioxide from nitrogen and methane, and light paraffins from light olefins (Kulprathipanja, 1998 and 2002).

2.2.2.1 Introducing zeolite as an adsorbent into polymer matrix

Gur (1994) fabricated zeolite NaX-polysulfone mixed matrix membranes by a melt extrusion process. Though, the effect of the filler was not observed. He concluded that the pore size of zeolite 13X was larger than the kinetic diameters of any of the gases studied. Therefore, separation due to sieving mechanism did not occur

Suer *et al.* (1994) prepared mixed matrix membranes of polyethersulfone, a glassy polymer, and hydrophilic zeolites 4A and 13X by using various membrane preparation procedures. The results showed that the permeabilities decreased up to 8 percent loading of zeolite 13X, and 25 percent loading for zeolite 4A before it increased for higher zeolite contents. They explained that the channel network grown-up as the zeolite loading increases in the polymer matrix, and consequently connects separate voids that offer an extra route for gas molecules. Normally, this led to an increase in the permeation of all gases with increasing zeolite loading in the mixed matrix membranes. Moreover, the polarity and adsorption of gases within the membrane matrix in addition to shape-selective and size-selective properties of the zeolite attributed to the transport property of gases across the zeolite in mixed matrix membranes. CO_2 molecules can interact with the polar surface of zeolite 13X and 4A during permeation and, thus, CO_2 permeability and permselectivity increase noticeably with increasing zeolite contents in the mixed matrix membranes.

Sukapintha (2000) examined the effect of PEG in a PEG-silicone rubber mixed matrix membrane for ethylene/ethane (C_2H_4/C_2H_6) separation. The results showed that PEG slows down the permeation rate of C_2H_4 and C_2H_6 in the membrane phase. However, the effect is more prevalent for C_2H_6 than C_2H_4. This facilitates the C_2H_4/C_2H_6 separation.

Tantekin-Ersolmaz *et al.* 189 (2000) studied the effect of zeolite particles on gas transport through mixed matrix membrane. They reported that the permeabilities of the silicalite-PDMS mixed matrix membranes increased with increasing zeolite particle size though the CO_2/N_2 permselectivities remained unaffected. The effect of particle size of zeolites was more prominent at the higher zeolite loading. They concluded that the permeability of gases through mixed matrix membranes decreased with increasing particle size, due to the increase in area and number of zeolite-polymer interfaces that the gas molecules need to move across.

Rattanawong (2001) prepared three types of MMM_{ADS} (silicalite-CA, NaX-CA, and AgX-CA) and evaluated them for propylene/propane (C_3H_6/C_3H_8) separation. To use as a reference, CA membranes were also made and tested. The results illustrated that C_3H_6/C_3H_8 selectivity decreases from silicalite-CA > CA >

NaX-CA > AgX-CA. This indicates that silicalite enhances the C_3H_6/C_3H_8 selectivity but NaX and AgX reverse the C_3H_6/C_3H_8 selectivity.

Pechar *et al.* (2002) prepared mixed matrix membranes of 6FDA-6FpDA-DABA and modified ZSM-2 zeolite by the solution casting method and characterized it by Fourier transform infrared spectroscopy (FTIR), transmission electron microscopy (TEM), and field emission scanning electron microscopy (FE-SEM). FESEM and TEM images did not reveal the presence of voids between the polyimide polymer and the zeolite. The performance of the mixed matrix membranes were tested by permeability measurements of He, O_2, N_2, CH_4, and CO_2 gases. The permeabilities of He, CO_2, and CH_4 all decreased, while O_2 and N_2 increased. All ideal permselectivities of O_2/N_2, N_2/CH_4, He/CO_2, and O_2/CO_2 separation were enhanced by using the mixed matrix membranes. However, the selectivity for CO_2/CH_4 decreased when compared to the pure 6FDA-6FpDA-DABA polyimide membrane.

Tin *et al.* (2005) investigated a carbon-zeolite mixed matrix composite membrane in which zeolite was a dispersed phase in a carbon matrix. The investigation was performed to study the use of zeolite KY as the dispersed phase in the continuous matrix phase of polyimide carbon membranes. A carbon-zeolite KY composite membrane was fabricated through the pyrolysis of a polymer-zeolite mixed matrix membrane. The results illustrated that the selectivity and permeability of the carbon-zeolite KY composite membrane increased to a great extent after carbonization. The carbon-zeolite KY composite membrane had higher separation performance in CO_2/CH_4 than the carbon membrane derived from a pure Matrimid® dense film (CM-Matrimid®-800). The selectivity of CO_2/CH_4 outstandingly enhanced from 61 to 124 for carbon-zeolite KY composite membrane, while the permeability decreased after carbonization, compared to CM-Matrimid®-800.

Chung *et al.* (2005 and 2006) prepared mixed matrix membranes by choosing polyethersulfone (PES) as continuous phase and zeolite 3A, 4A and 5A as dispersed phase. The results implied that using large pore zeolite for MMMs will potentially compensate the negative effects of partial pore blockage and polymer chain rigidification on permeability.

In 2006, Pechar and coworkers fabricated the mixed matrix mem-

branes composed of zeolite L dispersed in a 6FDA-6FpDA-DABA polyimide matrix and characterized it for gas separation performance. The interfacial contact between the zeolite and the polymer phase was improved by introducing an amine functional group on the zeolite surface and covalently linking them with carboxylic acid groups present along the polyimide backbone. The FTIR of the resultant mixed matrix membrane proved the presence of hydrogen-bonded amine and amide-link formation upon annealing. Moreover, the lack of an increase in permeability of He through the mixed matrix membrane as compared to the pure polyimide membrane, suggested that they were void-free at the polymer-zeolite interface. While the permeability of O_2 and N_2 in the membranes increased with the addition of zeolite L, these mixed matrix membrane did not give substantial selectivity improvements.

Fu *et al.* (2006) investigated the effect of 3-(trimethoxysilyl)propyl-methacrlate (TMOMPA) as a kind of compatibilizer to reduce the void between the zeolite-polymer interface. Zeolite 4A was chosen as a zeolite to embed in the poly-methymethacrylate (PMMA) polymer matrix. It was found that the O_2 permeability of zeolite-filled PMMA membranes was lower than pure PMMA membranes. In addition, the permeability of O_2 through the zeolite-filled PMMA membranes decreased with increasing zeolite 4A loading, up to 33.3 wt%. At the same zeolite composition, the zeolite surface modified with TMOPMA improved the solubility and diffusivity coefficients of zeolite-filled PMMA membranes, confirmed by SEM images, while the PMMA/4A showed lower permeability but higher selectivity.

Husain and Koros (2007) fabricated mixed matrix asymmetric hollow fiber membranes by spinning via a dry jet-wet procedure using a surface modified small pore size zeolite, HSSZ-13, incorporated in an Ultem® 1000 polyetherimide matrix. Due to poor adhesion between the zeolite and the polymer phase, silane coupling agents were firstly chosen as a method to improve the zeolite-polymer compatibility and subsequent polymer "sizing" did not increase the selectivity of the mixed matrix membrane. On the other hand, hollow fiber asymmetric membranes incorporating Grignard reagent-modified zeolite demonstrated a selectivity enhancement of 10%, 29%, and 17% for O_2/N_2, He/ N_2, and CO_2/CH_4 pure gas pairs, respectively, and 25% for mixed gas CO_2/CH_4.

Li *et al.* (2007) fabricated mixed matrix membrane from polyethersul-

fone (PES) as a continuous phase and NaA and AgA as a dispersed phase to study the effect of partial pore blockage and facilitated transport on CO_2 and CH_4 permeability. CO_2 and CH_4 permeability decrease with increasing zeolite loading. They found that facilitated transport can not overcome the negative effects of polymer chain rigidification and partial pore blockage of zeolite on CO_2 permeability since the kinetic diameter of CO_2 gas is very close to the pore size of AgA zeolite.

Tanupabrungsun (2007) studied the separation performance of NaX-CA, NaY-CA, and Silicalite-CA mixed matrix membranes, which were prepared by the solution casting method, for C_3H_6/C_3H_8 and CO_2/CH_4 separation. For the C_3H_6/C_3H_8, the results showed that the NaX-CA MMMs provided reverse selectivity, but the others expressed selectivity enhancement because the NaX-zeolite has more acid sites for adsorbing C_3H_6 than the NaY-zeolite and the silicalite. This is attributed to the stronger interaction and adsorption of C_3H_6. The effect of NaX-CA MMMs and NaY-CA MMMs on CO_2/CH_4 selectivity, investigated by pure gas measurement, suggested that CO_2 was more adsorbed into NaX-CA MMM and NaY-CA MMM than into silicalite-CA MMM because silicalite has very high Si/Al ratios and is very hydrophobic, but NaX and NaY have strongly polar anionic frameworks and strong local electrostatic fields. This caused the enhancement of CO_2 solubility in both NaX-zeolite and NaY-zeolite added to the mixed matrix membranes.

2.2.2.2 Introducing other materials as an adsorbent into polymer matrix

Vu *et al.* (2003) incorporated a carbon molecular sieve (CMS) as the disperse phase in mixed matrix membrane films using two different continuous polymer matrices (Matrimid® 5218 polyimide and Ultem® 1000 polyetherimide). The CMSs were prepared by the pyrolysis of a Matrimid® polyimide precursor to the final temperature of 800°C. Mixed matrix films containing a high loading of CMS particles (up to 35 wt. %) dispersed within the Matrimid® 5218 polyimide and the Ultem® 1000 polyetherimide polymer matrix were prepared by the flat-sheet solution casting method. The results showed that the Matrimid®-CMS and Ultem®-CMS mixed matrix membranes displayed significant enhancement in CO_2/CH_4 selectivity, about 45 and 40% respectively compared to the pure polymer.

Anson *et al.* (2004) investigated the performance of various novel

mixed matrix membranes for CO_2/CH_4 separation as a function of carbon loading. Acrylonitrile-butadiene-styrene (ABS) copolymers were used as the polymer matrix and two micro-mesoporous activated carbons (AC) were chosen as inorganic fillers. The results showed that the pure gas permeabilities and CO_2/CH_4 selectivities of ABS-AC mixed matrix composite membranes are simultaneously increased with increasing activated carbon loadings in the mixed matrix composite membrane, compared to that of the intrinsic ABS polymeric membranes.

Sridhar *et al.* (2006) developed modified poly(phenylene oxide) (PPO) membranes to improve the gas permeability characteristics of high-performance PPO membranes for the separation of CO_2/CH_4 gaseous mixtures. PPO was successfully modified physically by the incorporation of heteropolyacid (HPA) filler and chemically by sulfonation. Incorporation of inorganic fillers into the PPO matrix as well as modication by sulfonation rendered the polymer amorphous. Modified PPO membranes showed good potential for the separation of CO_2 from CO_2/CH_4 gaseous mixtures by increasing the CO_2 selectivity over the pristine PPO membranes. Cong *et al.* (2007) explored the use of carbon nanotubes (CNTs) in order to enhance the mechanical strength of polymeric membranes. The single-walled CNTs (SWNTs) and multi-walled CNTs (MWNTs) incorporated into a brominated poly(2,6-diphenyl-1,4-phenylene oxide) ($BPPO_{dp}$) matrix increased CO_2 permeability, but CO_2/N_2 selectivity did not improve. The pristine CNT-enhanced gas permeability was attributed to the nanogaps which formed surrounding the CNTs. Hence it is practicable to add CNTs into the polymer matrix for enhanced mechanical strength without deteriorating the gas separation performance of the membranes.

Kim *et al.* (2007) fabricated and characterized novel nano-composite membranes containing modified SWNTs inside a polysulfone matrix. To help the dispersion in the polysulfone, the carbon nanotubes were functionalized with long chain alkyl amines. Both permeabilities and diffusivities of the membranes increased with the weight fraction of carbon nanotubes at 4 atm.